Distribution of chain defects and microstructure of melt crystallized polyethylene

F. J. Baltá Calleja, J. C. González Ortega and J. Martinez de Salazar
Instituto de Estructura de la Materia, CSIC, Madrid 6, Spain
(Received 28 February 1978; revised 11 April 1978)

A combined study using wide-angle X-ray diffraction (WAXD) and small-angle X-ray diffraction (SAXD) of a series of mostly low density polyethylenes with a wide range of chain defect concentrations (0.1–7%) crystallized from the melt is reported. The data presented here complement the earlier results obtained by Swan[7] and Holdsworth and Keller[8] for copolymers. The concurrent unit cell expansion and long period decrease with increasing chain defect concentration leads to a picture of chain defects (branches, unsaturations) being distributed between the crystalline lamellae and the surface layer. Based on a model which assumes inclusion of defects within the lattice by means of a generation of $2g$l kinks, (supported by the parallel increase of paracrystallinity) an estimation of the concentration of chain defects, ϵ_c, incorporated into the crystal lattice (<1%) is attempted. The density of defects in the non-crystalline regions, ϵ_a, turns out to be substantially larger than ϵ_c and supports the view of a clustering of defects. ϵ_c and ϵ_a are both increasing functions of ϵ with a tendency to level off for $\epsilon > 6$. According to this model, the fraction of defects incorporated into the lattice does not exceed 20% of the total number of defects in any of the samples investigated. The fraction of defects excluded from the lattice (>80%), on the other hand, sets a higher permissable limit to the crystal thickness value achieved.

INTRODUCTION

The capability of chain defects (in the form of branches, unsaturations, comonomer units) to become incorporated into the crystal lattice of polyethylene (PE) as interstitial imperfections has been a topic of considerable controversy. While thermodynamic[1–3] and some structural treatments[4] suggest the exclusion of defects from the crystalline regions, the unit cell expansion of bulk[5–7] and solution crystallized material[8] has been interpreted as firm evidence of the incorporation of defects within the lattice. Such an inclusion of defects within the lattice, on the other hand, does not exclude the location of a certain fraction of these defects in the disordered surface layer. The major problems arising in this case are: (1) the evaluation of the defect distribution between crystalline regions and the crystal surface and (2) the specific way in which these interstitial imperfections are located in the lattice without causing their destruction.

The accommodation of chain defects within the lattice of various polymers and copolymers through formation of conformational chain isomers was first suggested by Vonk[9,10] on the basis of X-ray diffraction studies, and further supported by Martuscelli[11] on morphological and thermodynamic grounds. According to these authors the chain defects can be placed at interstitial (kinks) and/or at substitution sites (jogs) in the crystal lattice.

The present work was undertaken in order to obtain further experimental evidence concerning this problem and, based on the above concepts, it attempts to offer a possible route for the assessment of the concentration of defects within the PE crystalline lamellae. For this study the variation of crystal thickness as derived from the X-ray long period and unit cell parameters is reported as a function of defect concentration. The present data complement the earlier results of Swan[7] and Holdsworth and Keller[8] on the expansion of unit cell parameters with ϵ, and in addition illustrate the influence of the defect concentration on crystal thickness, thus supporting the view of a concurrent defect rejection. The attempt to calculate defect inclusion in the lattice indicates that most of the defects are excluded from the lattice.

EXPERIMENTAL

Materials

A series of commercial polyethylenes with a wide range of chain defects (from 0.17 to 7%) and average molecular weights were investigated (see *Table 1*). The same samples have been investigated in other studies[12–15]. According to infra-red spectroscopy measurements the lateral branches attached to the main chain are butyl or longer methylene sequences[13,16]. The concentration of branches was determined from the absorbance of the methyl symmetrical deformation band at 1378 cm^{-1}. The contribution of unsaturations (bands at 960 cm^{-1}, vinylene; 903 cm^{-1}, vinyl; 888 cm^{-1}, vinylidene) was also taken into account[13]. The total number of defects, ϵ, is given as the sum of branches plus unsaturations and includes chain ends as well. The samples were melted at 150°–160°C in evacuated glass tubes in the presence of a nitrogen atmosphere. They were subsequently transferred to a bath at ~2°C below each melting point for 72 h and finally cooled at a rate of about 1°C/min. From the samples thus obtained slices of 0.5–

0032–3861/78/1909–1094$02.00

Table 1 Molecular weight, defect concentration, X-ray crystallinity, long period, crystal thickness, macroscopic density and unit cell density

Sample	$M_W \times 10^{-3}$	ϵ(%)	α(%)	L (Å)	l (Å)	ρ(g/cm^3)	ρ_c(g/cm^3)
1	–	0.17	0.89	257	224	0.9775	0.998
2	150	0.19	0.86	260	219	0.9800	1.000
3	50	0.28	0.78	168	129	0.9799	0.998
4	245	0.93	0.82	215	170	0.9603	0.995
5	10	1.21	0.72	202	141	0.9537	0.993
6	51	1.76	0.70	184	124	0.9485	0.991
7	53	2.53	0.61	196	113	0.9337	0.986
8	10	2.57	0.62	193	115	0.9404	0.986
9	1.5	2.63	0.67	205	131	0.9435	0.986
10	2.5	2.89	0.65	209	128	0.9325	0.985
11	1.5	3.25	0.68	192	124	0.9355	0.984
12	5.6	3.49	0.66	205	128	0.9348	0.985
13	10	3.61	0.50	142	66	0.9150	0.983
14	6.0	4.63	0.53	123	60	0.9142	0.986
15	7.0	4.77	0.37	138	47	0.9073	0.980
16	3.7	6.90	0.28	150	39	0.8968	0.976

1.0 mm thickness were cut to about 10 x 10 mm in size for the X-ray diffractometer. The surfaces were ground flat with emery paper and carefully aligned on the axis of the diffractometer.

Techniques

Wide-angle X-ray diffractograms were obtained at room temperature using a Ni-filtered CuKα radiation from a tube (40 kV, 24 mA). Optimum working conditions for the diffractometer were selected according to a previous systematic study of the PE line profiles[17]. One degree divergence and antiscatter, and 0.1 mm receiving slits were used and radiation was detected with a proportional tube, pulse height analyser and counter. The polyethylene diffraction peaks (110), (200) and (020), scanned at a rate of 1°(2θ)/min and recorded on chart paper moving at 20 mm/min, were used to calculate the unit cell dimensions a and b. Correction for the position of the diffraction peaks due to absorption was not necessary since the variation of the absorption coefficient with ϵ lies within the error of experiment. The standard deviation was found to be 0.01 Å. The unit cell edge c, was assumed equal to 2.54$_6$ Å[7,18]. The samples investigated exhibited no orientation. The volume crystallinity, α, was calculated with the help of a computer program by least square fitting[19]. This program makes use of a combination of Lorentz–Gauss functions and enables a systematic separation of crystalline peaks and 'amorphous' halo. The crystallinity values obtained show a good correlation with those derived from density measurements.

Long periods were obtained by applying Bragg's law to the maxima from small-angle X-ray diffraction (SAXD) recorded photographically with pinhole collimation and filtered CuKα radiation from a rotating anode source (40 kV, 100 mA). The positions of the maxima were measured both visually on a film reader and photometrically. The crystal thickness dimension, l, was calculated with the first maximum (larger long period) reduced by the volume fraction of crystallinity according to the method of Illers and Hendus[20].

The density, ρ, of the samples was determined by the column gradient method. The liquid used was a mixture of p-xylene (83%) and carbon tetrachloride (17%). The density measurements are believed to be accurate to ±0.0005 g/cm^3. The crystalline density, ρ_c, was derived from unit cell dimensions. The standard errors in all dimensions correspond to a standard deviation of 0.001 g/cm^3.

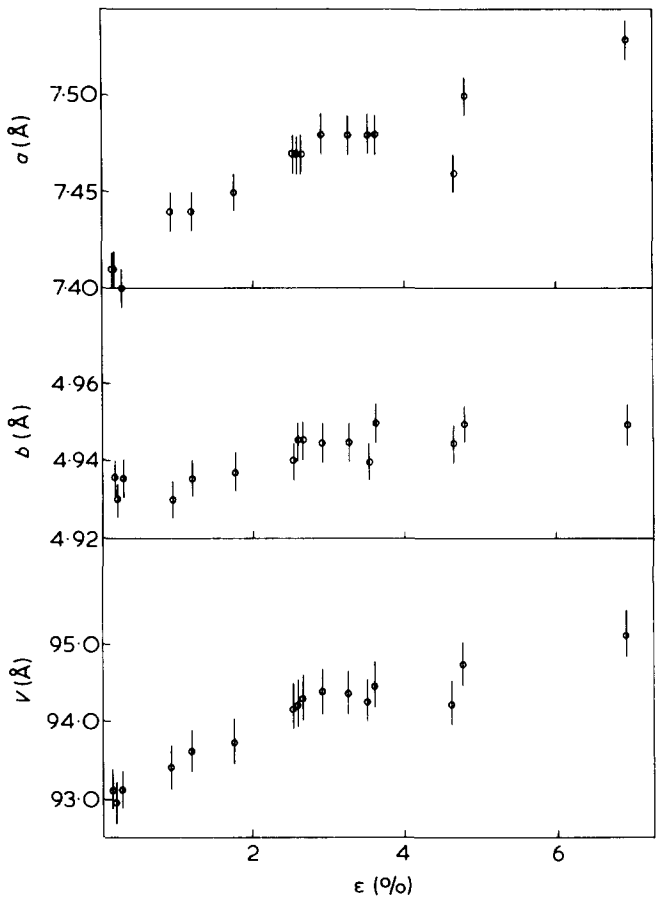

Figure 1 Expansion of unit cell dimensions a and b and unit cell volume for melt crystallized PE with various defect concentrations

RESULTS

The expansion of the parameters a and b and the unit cell volume V is illustrated in *Figure 1* as a function of increasing percent of total number of defects ϵ. The unit cell edge, c, was assumed to be equal to 2.54$_6$ Å and independent of ϵ[17,18]. The a dimension increases continuously in the investigated range of ϵ. The b dimension, on the other hand, expands only slightly from ϵ = 0 to 3% and thereafter remains practically constant. This behaviour is similar to that reported by Swan for ethylene–propylene copolymers[7]. From the trend obtained with the parameters a and b, the unit cell

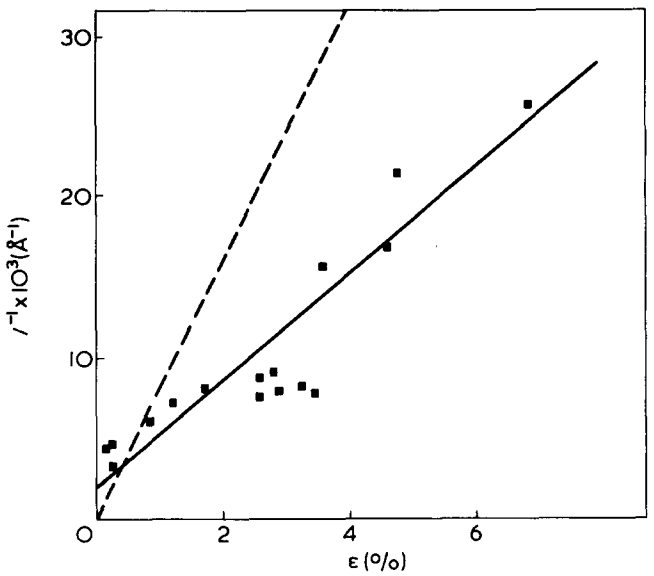

Figure 2 Plot of reciprocal crystal thickness vs. defect concentration. – – – –, Represents the ideal case of a periodic ϵ^{-1} distribution of defects assuming that only the chain sequences free of defects are allowed to crystallize

volume, V, shows, as a result, a fast initial increase up to $\epsilon = 3\%$ and then a tendency to level off for $\epsilon > 3\%$. It is interesting to note that the overall increase of V is independent of the molecular weight of the samples.

The SAXD patterns of the investigated samples are characterized by the presence of one (L_1) or eventually two (L_1 and L_2) diffraction rings with no tangential intensity variation. The intensity of L_2 is much weaker than that of L_1 and the ratio $L_1/L_2 \sim 1.8$. We are aware of some of the uncertainties associated with the interpretation of these two diffraction maxima[20,21]. However, since L_2 appears in only five of the samples, the long period, L, was derived from L_1. The values of L, l, α, ρ, and ρ_c are presented in *Table 1* as a function of increasing ϵ. L and, as a consequence, $l = L\alpha\rho/\rho_c$ (assuming a two-phase structure), show a decreasing tendency with increasing ϵ. The clear decreasing influence of ϵ on L for quenched PE was previously reported by one of us[22]. *Figure 2* illustrates the plot of l^{-1} vs. ϵ which for the present data yields a variation of type $l^{-1} = l_0^{-1} + K\epsilon$ with an axial intercept $l_0^{-1} \approx 1.87 \times 10^{-3}$ Å^{-1} and a slope $K = 3.1 \times 10^{-3}$ Å^{-1} per ϵ unit. The broken line in *Figure 2* illustrates for comparison the ideal case of a periodic distribution of chain defects corresponding to an average distance between two consecutive branches $l = \epsilon^{-1} \times 1.27$ Å. Such a distribution assumes a defect exclusion from the crystals.

DISCUSSION

Branching influences firstly the packing of the chains within the crystals causing the observed expansion of the crystalline lattice. The higher the total number of defects, the more defects seem to be accommodated within the lattice. Secondly it severely affects the crystal thickness values (see *Figure 2*). The correlation obtained deviates from a periodic ϵ^{-1} distribution of defects, suggesting that branches either penetrate within the lattice or that they occur in the form of clusters. Chain ends are considered as defects in this approach and as such are included in the ϵ value, as mentioned above. Evidence[23] indicates that a substantial portion of ends can be situated on the crystal surface in the form of cilia.

While the expansion of the unit cell with ϵ favours an increasing incorporation of defects within the lattice the observed decrease of crystal thickness with ϵ suggests, on the contrary, a gradual rejection of defects from the crystals. The latter is, in addition, consistent with the simultaneous observed decrease of crystallinity (proportional to l/L) with ϵ. This favours the location of crystallinity deficiency at the crystal surfaces. Incorporation of branches within the lattice might nevertheless contribute likewise to a certain extent to the formation of 'amorphous' defects in the crystal[8]. The present apparently contradictory results are, however, compatible if one accepts that defects are distributed not only within crystalline cores but also outside of them.

Concerning the observed unit cell expansion it can be assumed that chain defects are mainly located at interstitial positions. This may very well occur, as suggested by Vonk[9,10] and as pointed out above, through the generation of 'kinks' (chain conformers) which originate around these chain chain defects. Conformational defects in the chain are, on the other hand, the main cause of the occurrence of paracrystalline distortions[24,25]. These paracrystalline distortions in PE increase with branching[26], thus supporting the concept of accommodation of branches within the lattice through kink generation. A rough calculation of the concentration of defects within the lattice may be attempted using the above ideas. Let us first assume that each chain defect within the lattice at an interstitial position originates a $2g1$ kink (*Figure 3*). This is the most abundant conformation (gtg) in PE crystals. According to Blasenbrey and Pechold[27]

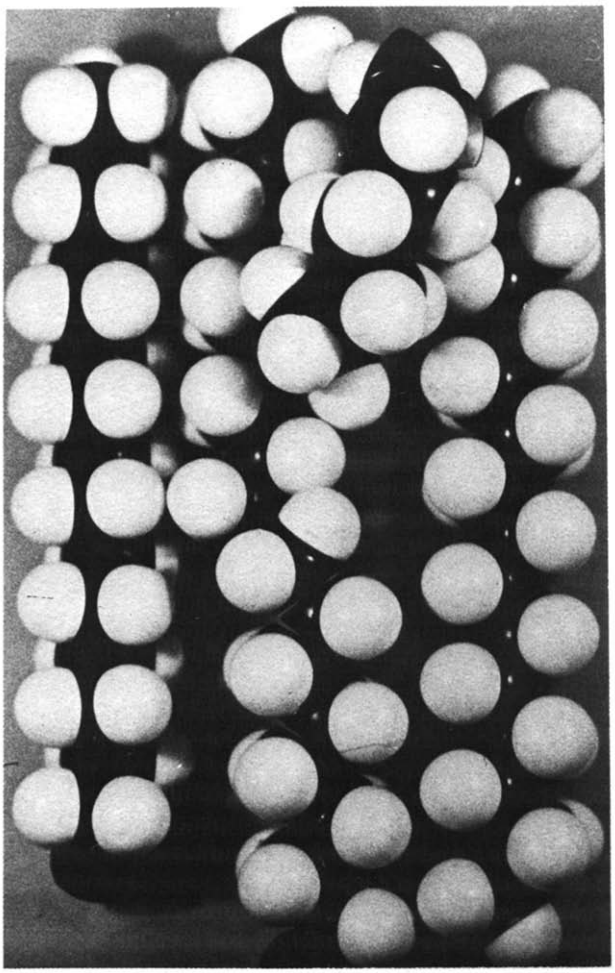

Figure 3 Model of a chain defect located at a $2g1$ kink on the (110) lattice plane

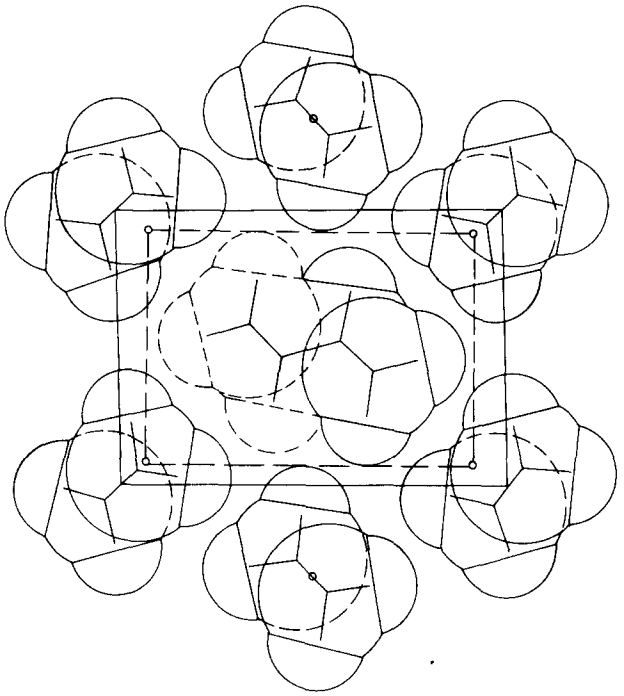

Figure 4 Unit cell expansion (from broken to full line) in PE due to a 2*g*l kink (after Scherr *et al.*[28])

the concentration of other kinks and jogs is much smaller and can consequently be neglected. The expansion in the basal plane of the unit cell due to the 2*g*1 kink is depicted in *Figure 4*. This expansion provides enough room for the accommodation of a branch in the unit cell. Local distortion which falls off gradually with distance in the lattice, causes a lateral displacement of the neighbouring molecules as illustrated by the model in *Figure 3*, resulting in an overall expansion of the crystal. This effect causes first a change of spacing due to the unit cell expansion and secondly a broadening of the diffraction lines due to the loss of long range order within the crystalline lattice[24] (paracrystalline distortions).

Let ΔV be the excess volume of a kink associated with a CH_2 group in the crystal. Let us further assume that v_0 is the volume occupied by a CH_2 group in an ideal crystal and that K is the concentration of kinks per 100 carbon atoms. The average volume v_K of a CH_2 unit in a crystal with a concentration of kinks, K, may then be expressed as:

$$v_K = K(v_0 + \Delta V) + (1 - K)\, v_0$$

thus,

$$K = \frac{v_K - v_0}{\Delta V} \qquad (1)$$

Since for each chain defect (branch or unsaturation) we impose the condition that it must be accommodated within a kink, the average volume v_ϵ occupied by a defect can be roughly assumed to be equal to v_K. Hence, the concentration of chain defects incorporated in the lattice per 100 carbon atoms, ϵ_c, will be nearly equal to K*. Since the unit cell volumes V_0, for $\epsilon = 0$, and V_ϵ, for a defect concentration ϵ are respectively equal to $V_0 = 4v_0$ and $V_\epsilon = 4v_\epsilon$ the fraction of chain defects per 100 atoms within the crystal lattice will be:

$$\epsilon_c \approx \frac{V_\epsilon - V_0}{4\Delta V} \qquad (2)$$

According to Pechold *et al.*[28,29] $\Delta V \sim 60$ Å^3. Thus, from the V_ϵ data of *Figure 1* and equation (2) an estimation of the proportion of defects ϵ_c within the crystal lattice of PE can be made. *Figure 5* illustrates the increase in the concentration of incorporated defects, ϵ_c, as a function of total concentration of defects in the PE chains. According to the data these highly branched PE samples ($\epsilon \sim 7\%$) may reach inclusions of the order of up to one defect every 100 carbon atoms in the crystal. This relatively small amount of defects is sufficient to account for the observed expansion of the lattice. It is interesting to compare these results with the three-dimensional concentration of 2*g*1 kinks, γ, directly derived from the paracrystalline distortions occurring in the (110) planes (equation 27, ref 24). *Table 2* illustrates the parallel increase of the paracrystalline factor, g_{110}, the concentration of 2*g*1 kinks, γ, and the inclusion of defects, ϵ_c, for three selected values of ϵ, and supports the trend of the results shown in *Figure 5* (ref 30).

If defect inclusions of less than one defect every 100 carbon atoms within the lattice are sufficient to account for the observed lattice expansion, the density of chain defects excluded from the lattice – mostly localized at the interlamellar disordered regions – will clearly be substantially

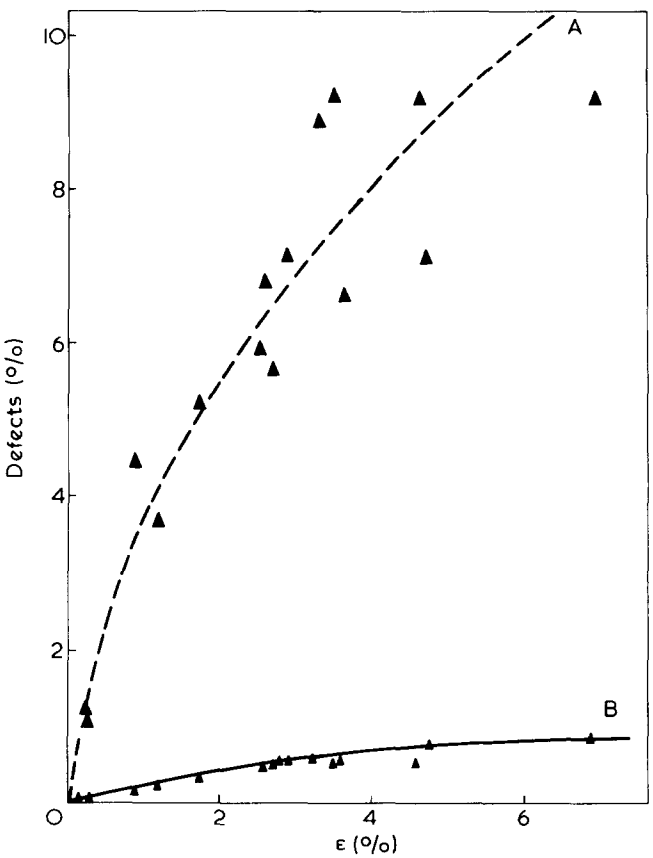

Figure 5 Density of defects in the crystals, ϵ_c (from equation 2) and in the 'amorphous' regions, ϵ_a, as a function of ϵ. A, ϵ_a; B, ϵ_c

* The total number of kinks in the crystal will be equal to the sum of the background concentration of kinks, K_0, plus an additional number of kinks, K, generated by inclusion of chain defects in the crystals. Thermodynamic calculations[25] predict a kink density, K_0, of ~0.06% for linear PE at room temperature. This small concentration K_0 contributes to the v_0 value but does not affect the calculation of ϵ_c.

Table 2 Concentraiton γ of $2g1$ kinks in the PE crystal lattice derived from the paracrystalline factor g in the (110) direction as compared with the chain defect inclusion ϵ_c (from equation 2) for three values of ϵ

ϵ(%)	g_{110}(%)	γ(%)	ϵ_c(%)
0.17	0.88	0.06	0.04
0.64*	1.4	0.16	–
6.90	2.99	0.72	0.93

* Value quoted from reference 23

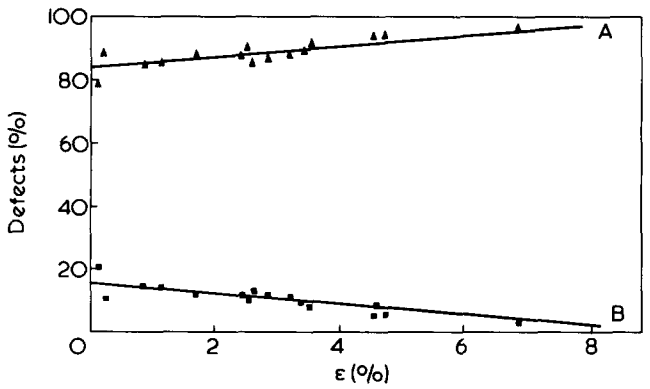

Figure 6 Fraction of defects in the crystalline, $\chi_c = \epsilon_c\alpha/\epsilon$ and in the 'amorphous' regions, $\chi_a = \epsilon_a(1-\alpha)/\epsilon$ as a function of ϵ. A, χ_a and B, χ_c

higher. This concentration of defects, ϵ_a, can be straightforwardly derived from the total amount of molecular defects per unit volume:

$$\epsilon = \alpha\epsilon_c + (1-\alpha)\epsilon_a;\ \epsilon_a = (\epsilon - \alpha\epsilon_c)/1-\alpha \tag{3}$$

It is evident that the low density of defects incorporated into the crystals imposes an overcompensating larger branching concentration in the amorphous layer. *Figure 5* illustrates the much faster increase of ϵ_a with ϵ where $\epsilon_a > \epsilon$.

So far we have discussed the concentration of defects within the crystals, ϵ_c, and in the 'amorphous' regions, ϵ_a, and we conclude that $\epsilon_c \ll \epsilon_a$. Most revealing, however, is the evaluation of the fraction of defects included in the lattice for each ϵ value. This fraction can be simply defined as

$$\chi_c = \frac{\epsilon_c\alpha}{\epsilon} \tag{4}$$

Similarly, the fraction of defects ejected from the lattice will be:

$$\chi_a = 1 - \chi_c = \frac{\epsilon_a(1-\alpha)}{\epsilon} \tag{5}$$

Figure 6 illustrates the plot of χ_c and χ_a vs. ϵ. These data show conclusively that for all ϵ values, $\chi_a \gg \chi_c$. In other words, the majority of defects (80–95%) are excluded from the lattice in all the samples investigated. Secondly, the data show that χ_a itself increases with ϵ, whereas χ_c decreases linearly with ϵ. This means, in addition, that the larger the total number of defects the higher the relative fraction of defects which tend to be excluded from the lattice. For the hypothetical case $\epsilon > 10\%$, $\chi_a \approx 100\%$ and $\chi_c \to 0\%$. The data of *Figure 6* may at first sight be misleading since they show relatively larger χ_c fractions at the lower end of ϵ. However, since ϵ is a very small quantity the actual density of defects ϵ_c is also extremely low as shown in *Figure 5*. In order to clarify this concept *Figure 7* schematically illustrates the prevailing exclusion of defects from the crystals for two samples of linear ($\epsilon = 0.17\%$) and conventionally branched PE ($\epsilon = 2.53\%$), respectively. Branching thus has a most dramatic effect on the density of defects ϵ_a within the amorphous layer. The shift[19] in the position of the 'amorphous' X-ray diffraction halo with increasing ϵ (from 21° for $\epsilon \sim 1\%$ to 19.5° (2θ) for $\epsilon \sim 7\%$), supports the above interpretation, indicating that the average interchain separation in the 'amorphous' regions gradually increases with the number of defects entering this layer. The high values obtained for ϵ_a apparently conflict with the conclusions drawn for solution-grown copolymer crystals[8,11]. According to these studies the thickness of the crystals is determined only by supercooling, irrespective of the distribution of defects in the chain. This discrepancy from our results may be partly due to the fact that the samples used in the present study were primarily low density PEs – branching occurring in clusters[31] – whereas the samples referred to in the above studies were copolymers with branches presumably distributed at random. The large values of ϵ_a, especially for $\epsilon > 3\%$, thus favour the existence of clusters of defects. A clustering of defects, suggesting the existence of tree-like branched structures and comb-like branching, has been recently shown in physical studies on low density PE[32]. The extremely low α values obtained for the highly branched samples suggest, in addition, the possibility of a breakdown of the two-phase model for the more defective samples[15].

Since the majority of defects are excluded from the lattice and these defects presumably set an upper limit to the crystal thickness it would then be reasonable to expect a decreasing dependence of l on χ_a. The data shown in *Figure 8* confirm this assumption. The least square plot of l vs. χ_a yields an excellent linear decrease according to:

$$l = l' - m\chi_a \tag{6}$$

where $m = 11.8$ Å/χ_a unit is the slope of the plot and $l' \sim$

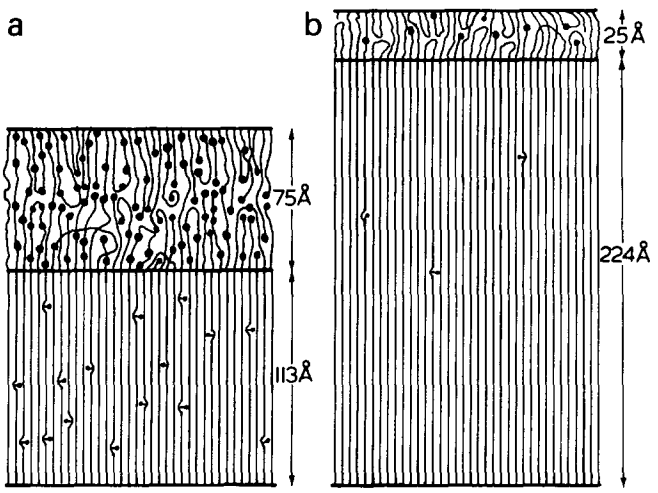

Figure 7 Schematic representation of the distribution of chain defects between crystalline lamellae and 'amorphous' layers for 2 samples with: (a) $\alpha = 60\%$, $\chi_a = 88\%$, $\chi_c = 12\%$, $\epsilon_a = 5.69$; $\epsilon_c = 0.51$; $\epsilon = 2.53$ and (b) $\alpha = 90\%$, $\chi_a = 79\%$, $\chi_c = 21\%$, $\epsilon_a = 1.22$; $\epsilon_c = 0.04$; $\epsilon = 0.17$

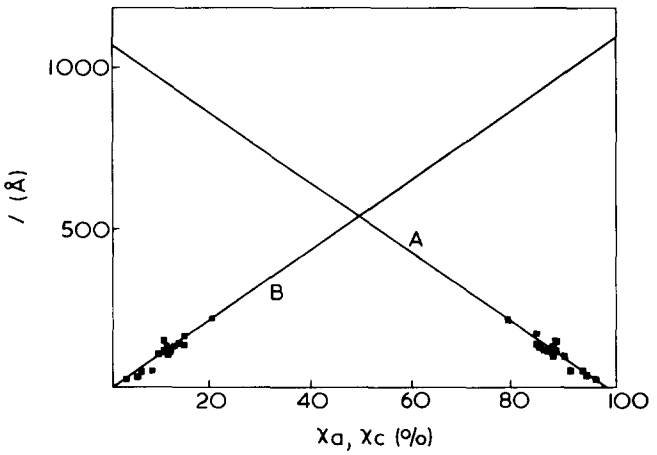

Figure 8 Plot of crystal thickness vs. χ_a and χ_c. A, χ_a; B, χ_c

1100 Å is the intercept value. The data of *Figure 6* clearly show that χ_a cannot reach values near $\chi_a = 0\%$. For the present samples this excludes the unrealistically high value $l' \sim 1100$ Å. The lowest reasonable values of χ_a for $\epsilon \to 0$ presumably lie close to 70–80% (see *Figure 6*). As a result this sets an upper limit for the thickness of PE crystals with no defects near 350 Å; this value is consistent with the value of l_0 in *Figure 2*. The region $0 < \chi_a < 0.5$ in *Figure 8* represents an ideal case where $\chi_a < \chi_c$, i.e. it would feature a model of preferential inclusion of defects within the lattice. The l values are evidently a function of crystallization conditions too. For example we have obtained lower values for the same set of samples quenched at 0°C: $m = 5.8$ Å and $l' \sim 600$ Å. Crystal thickness thus depends also on supercooling, as expected[8,11]. From $\chi_a = 100\%$ (i.e. $\epsilon \sim 10\%$ in *Figure 6*) one derives, on the other hand, a value $l \to 0$, that is to say, consistent with a total absence of crystallinity. *Figure 8* illustrates the relative linear increase obtained for the fraction χ_c of defects incorporated into the lattice with l as χ_a decreases.

CONCLUSIONS

The present results suggest that the expansion of the unit cell for the melt crystallized PE samples investigated can be satisfactorily explained assuming that the occurrence of chain conformations $2g1$ capable of accommodating a fraction of molecular defects (branches, unsaturations) within the lattice is smaller than, say, 20% (for the less defective samples) of the total concentration of defects. The remaining percentage of defects which is, therefore, larger than 80% is probably rejected from the lattice and, under the crystallization conditions used, controls the crystal thickness according to equation (6). These results seem to agree with theories[1,33] predicting a major exclusion of defects from the lattice, thus mainly allowing chain sequences, free or with a minimum of defects, to crystallize. We wish to emphasize, however, that the conclusions reached do strictly apply to the present series of PE samples which were crystallized during cooling. Further experiments on isothermally crystallized branched materials would be required to demonstrate the generality of the conclusions in a wider sense.

ACKNOWLEDGEMENTS

The work performed by one of us (J. M. S.) was generously supported by a grant from FPI.

REFERENCES

1 Flory, P. J. *Trans. Faraday Soc.* 1955, **51**, 848
2 Richardson, M. R., Flory, P. J. and Jackson, J. B. *Polymer* 1963, **4**, 221
3 Kilian, H. G. *Kolloid Z. Z. Polym.* 1965, **202**, 97
4 Kawai, T., Ojihara, K. and Maeda, H. *Makromol. Chem.* 1970, **132**, 87
5 Eichorn, R. M. *J. Polym. Sci.* 1958, **31**, 197
6 Cole, E. A. and Holmes, D. R. *J. Polym. Sci.* 1960, **46**, 245
7 Swan, P. R. *J. Polym. Sci.* 1962, **56**, 409
8 Holdsworth, P. J. and Keller, A. *J. Polym. Sci. (Polym. Lett. Edn)* 1967, **5**, 605
9 Vonk. C. G. presented at the *8th Prague 'Microsymposium on Macromolecules Morphology of Polymers'*, August, 1971
10 Kortleve, G., Tuijnman, C. A. F. and Vonk, C. G. *J. Polym. Sci. (A-2)* 1972, **10**, 123
11 Martuscelli, E. *J. Macromol. Sci. (B)* 1975, **11**, 1
12 Baltá Calleja, F. J. and Rueda, D. R. *Polym. J.* 1974, **6**, 216
13 Rueda, D. R., Baltá Calleja, F. J. and Hidalgo, A. *Spectrochim. Acta (A)* 1974, **30**, 1545
14 Baltá Calleja, F. J. *Colloid Polym. Sci.* 1976, **154**, 158
15 Rueda, D. R., Baltá Calleja, F. J. and Hidalgo, A. *J. Polym. Sci. (Polym. Phys. Edn)* 1977, **15**, 2027
16 Rueda, D. R., Baltá Calleja, F. J. and Hidalgo, A. *C. R. Acad. Sci. (Paris)* in press
17 Gonzalez Ortega, J. C. and Baltá Calleja, F. J. *An. Fis.* 1974, **70**, 92
18 Davies, G. T., Eby, R. K. and Martin, G. M. *J. Appl. Phys.* 1968, **39**, 4973
19 Martinez de Salazar, J., González Ortega, J. C. and Baltá Calleja, F. J. *An. Fis.* 1977, **73**, 244
20 Illers, K. H. and Hendus H. *Kolloid Z.* 1967, **218**, 56
21 Geil, P. H. *J. Polym. Sci. (C)* 1966, **12**, 149
22 Peterlin, A. and Baltá Calleja, J. F. *Kolloid Z.* 1970, **242**, 1093
23 Keller, A. and Priest, D. J. *J. Polym. Sci. (Polym. Lett. Edn)* 1970, **8**, 13
24 Čačkovič, H., Hosemann, R. and Wilke, W. *Kolloid Z.* 1969, **234**, 1000
25 Hosemann, R. *CRC Crit. Rev. Macromol. Sci.* 1972, October, 351
26 Hoseman, R. and Wilke, W. *Macromol. Chem.* 1968, **118**, 230
27 Blasenbrey, S. and Pechhold, W. *Ber. Bunsenges Phys. Chem.* 1970, **74**, 784
28 Pechhold, W. *Kolloid Z.* 1968, **228**, 1
29 Scherr, H., Pechhold, W. and Blasenbrey, S. *Kolloid Z. Z. Polym.* 1970, **238**, 396
30 Martinez de Salazar, J. and Baltá Calleja, F. J. unpublished results
31 Kasey, K., Elston, C. T. and Phibbs, M. K. *J. Polym. Sci. (Polym. Lett. Edn)* 1964, **2**, 1053
32 Kunn, R., Krömer, H. and Rossmanith, G. *Angew. Makromol. Chem.* 1974, **40/41**, 361
33 Čačkovič, H., Loboda-Čačkovič, Hosemann, R. and Weick, D. *Colloid Polym. Sci.* 1974, **252**, 812